# DEVELOPMENT OF HIGH-PERFORMANCE LONG-PULSE DISCHARGE IN KSTAR

Hyun-Seok Kim Korea institute of Fusion Energy (KFE) Daejeon, Republic of Korea Email: hskim0618@kfe.re.kr

YoungMu Jeon, Hyunsun Han, Kimin Kim, KwangPyo Kim, Heungsu Kim, Tongnyeol Rhee, Juhyung Kim, Junghee Kim, Dongcheol Seo, Eunnam Bang, Hee-Jae Ahn, Hyun-Sik Ahn, Jaesic Hong, Jinhyun Jeong, Jongdae Kong, Jong-Gu Kwak, Jongkook Jin, Jungyo Bak, Kaprai Park, Kyu-Dong Lee, Mi Joung, Sang Woo Kwag, Sang-Hee Hahn, Si-Woo Yoon, Sonjong Wang, Woong Chae Kim, Young-Ok Kim, and KSTAR teams Korea institute of Fusion Energy (KFE)

Daejeon, Republic of Korea

SangKyeun Kim Princeton Plasma Physics Laboratory Princeton, United States of America

#### **Abstract**

Developing high-performance long-pulse scenarios in tokamaks requires solving several critical challenges. In KSTAR, three major challenges have been systematically addressed to extend pulse duration. The first challenge is plasma-facing component (PFC) heat control. Excessive heating of the poloidal limiter, caused by fast ion orbit losses and beam shine-through, was mitigated by optimizing plasma shape and neutral beam injection composition. In addition, the temperature rise of the divertor was effectively resolved by installing and operating a tungsten monoblock divertor. The second challenge involves magnetic diagnostic reliability during long pulses. Signal drift of heated magnetic probes distorted equilibrium reconstruction, but a new thermal shielding protector significantly reduced this effect. The third challenge is long-time-scale performance degradation. Although high  $\beta$ P and good confinement were initially achieved, gradual reduction of  $\beta$ P was observed over current relaxation times and thousands of energy confinement times. This degradation is likely linked to persistent toroidal Alfvén eigenmodes and their cumulative impact on fast ion confinement. To mitigate these effects, we optimized long-time-scale gas fueling scenarios to prevent the reduction of fast ion pressure. With these advances, KSTAR has demonstrated 102-second operation with  $\beta$ P~2.7,  $\beta$ N~2.1, H98y2~1.1, and fNI $\leq$ 0.96. These results mark a critical step toward establishing reactor-relevant long-pulse operational scenarios.

## 1. INTRODUCTION

Achieving long-pulse plasma operation in tokamaks is one of the most demanding challenges in the pursuit of fusion energy. A tokamak generates plasma current primarily through inductive means, relying on the current swing of poloidal field (PF) coils. This intrinsic dependence inherently restricts pulse duration due to the finite current capacity of the PF system. Nevertheless, sustainable long-pulse discharges are indispensable for demonstrating reactor-relevant operation and for moving toward economically viable fusion energy. The central requirement for such operation is to maximize the fraction of non-inductive current, fNI, defined as the ratio of non-inductively driven current INI to total plasma current IP. In practice, this is achieved by increasing the bootstrap current fraction, fBS, through high-pressure gradients, and by enhancing the externally driven current fraction, fCD, with optimized heating and current drive (H&CD) systems. Both components can be expressed as functions of the plasma pressure β, normalized beta βN, and dimensionless current drive efficiency ζCD. While raising auxiliary heating power PCD can enhance fCD, this can also reduce fusion gain Q, highlighting the importance of simultaneously achieving high confinement and efficient current drive. Equally important is the ability to sustain such a high-performance state over extended timescales, which requires managing two long characteristic times in tokamak plasmas: the evolution of the current density profile, typically on the order of 10-100 seconds, and plasma-wall interaction timescales, which can extend to hundreds of seconds. Thus, long-pulse discharges provide a critical platform not only to validate engineering design limits but also to expose physical processes that evolve slowly yet have cumulative impacts, such as impurity accumulation, diagnostic drift, and fast ion transport losses.

Recent experimental campaigns in devices such as DIII-D and EAST have advanced the frontier of high-performance long-pulse plasma operation. Joint DIII-D/EAST studies based on high- $\beta$ P operation have demonstrated remarkable progress toward fully non-inductive scenarios. In DIII-D, fully non-inductive operation was achieved with  $\beta$ P  $\geq$  3.0, fBS  $\geq$  0.8, and H98y2  $\approx$  1.5 for pulses lasting several seconds, with internal transport barrier (ITB) formation observed at large minor radius. In EAST, fully non-inductive discharges have been

realized with  $\beta P \approx 2.0$ , fBS  $\approx 0.5$ , and H98y2  $\approx 1.3$  for 60 seconds, complemented by the record 1056-second operation in super I-mode. These achievements demonstrate that long-pulse plasmas can be sustained with advanced control of H&CD systems and plasma—wall interactions. Building on this progress, KSTAR has pursued long-pulse operation since 2015, reporting up to 102-second high-performance discharges. Unlike EAST, KSTAR does not utilize lower hybrid current drive (LHCD), which has high  $\zeta$ CD efficiency, but instead employs neutral beam injection (NBI) and electron cyclotron heating (ECH), similar to DIII-D. This provides a unique platform to study fast ion confinement and NBI-driven pressure evolution under long-pulse conditions. In particular, maintaining fast ion confinement is essential for ITER and DEMO, where  $\alpha$ -particle losses could threaten both performance and machine protection. KSTAR experiments adopting high- $\beta$ P operation have demonstrated distinct physics compared to DIII-D, as ITB formation is absent, and performance improvement is instead linked to the suppression of toroidal Alfvén eigenmodes through optimized EC deposition.

In this paper, we present the development of long-pulse plasma scenarios in KSTAR, addressing key challenges related to PFC heat loads, diagnostic stability, and performance degradation on long timescales. The following sections detail the optimization of high-βP scenarios, experimental results from recent campaigns, and the implications for reactor-relevant operation.

#### 2. HIGH-PERFORMANCE LONG-PULSE SCENARIO IN KSTAR

#### 2.1. KSTAR high \( \beta \) operation scenario

A high  $\beta P$  discharge scenario was adopted in KSTAR to enhance the bootstrap current fraction,  $f_{BS}$ , and thereby support the development of long-pulse discharges. At relatively low plasma currents (IP = 400–500 kA), neutral beam injection (NBI) often drives strong toroidal Alfvén eigenmodes (TAEs), which lead to significant fast ion

transport and a consequent reduction in plasma total pressure. These TAEs pose a serious limitation on achieving and sustaining high  $\beta_P$  plasmas. However, recent KSTAR experiments have demonstrated that this can be mitigated or even suppressed by carefully controlled electron cyclotron wave (EC-wave) deposition. Such stabilization enhances fast ion confinement and enables access to improved performance regimes. This result emphasizes that, for KSTAR, achieving a high  $\beta P$  discharge requires precise control of wave deposition to regulate MHD activity.

As reported in earlier studies, the establishment of high  $\beta P$  discharges at KSTAR is highly sensitive to the location of electron cyclotron heating (ECH) and electron cyclotron current drive (ECCD) deposition. Specifically, deposition must be carefully aligned within a narrow region near the magnetic axis. For example, discharge #18602 achieved  $\beta P \approx 2.9$ , which is significantly higher than the  $\beta P \approx 2.2$  obtained in a reference H-mode discharge (#18597) under nearly identical operational conditions. The only distinction was in the toroidal field, with BT = 1.8 T for the high  $\beta P$  case and BT = 1.9 T for the reference case, which shifted the EC resonance and deposition. This small variation in BT resulted in a substantial performance difference, highlighting the strong sensitivity of high  $\beta P$  access to ECH/ECCD deposition.

Detailed comparisons between the two discharges further illustrate the benefits of controlled EC-wave deposition. As shown in the time traces, the high  $\beta P$  discharge exhibited approximately a 30% increase in  $\beta P$  and a 50% reduction in loop voltage  $(V_{loop})$  compared to the reference discharge. Neutron rate diagnostics confirmed enhanced fast ion confinement, which is consistent with suppression of TAEs by ECH/ECCD injection. Importantly, these improvements occurred without significant changes to other

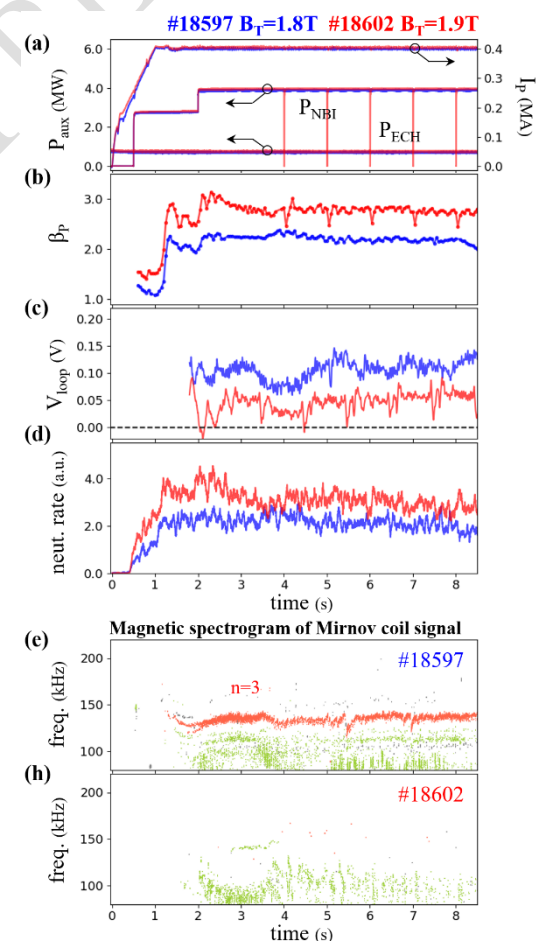


Fig. 1. Comparison of two similar discharges with different ECH/ECCD depositions. A high  $\beta_P$  discharge #18602 (red) was obtained by EC resonance line  $R_{res}\sim1.72$  m at BT=1.8 T, while a typical H-mode discharge #18597 (blue) was done by  $R_{res}\sim1.82$  m at BT=1.9 T.

operating parameters, such as plasma current, density, or NBI power.

Unlike the conventional high  $\beta P$  scenarios observed in DIII-D and EAST, where the formation of internal transport barriers (ITBs) by strong off-axis ECH/ECCD plays a dominant role, KSTAR's high  $\beta P$  regime relies on near on-axis ECH/ECCD. Consequently, ITB formation is not observed, yet  $\beta P$  is significantly increased through fast ion stabilization and current drive effects near the magnetic axis.

#### 2.2. Heat control of PFCs

In KSTAR, protection of plasma-facing components (PFCs) during long-pulse operation is ensured by dedicated interlock systems that monitor thermocouple signals at 1 Hz. Thermocouples are embedded 5 mm below the surface of the tiles, their readings underestimate the true surface temperature. For example, in discharge #21735, terminated at 89 s, infrared thermography (IRTV) measured a surface temperature of 1182 °C at the poloidal limiter, while the thermocouples registered only 609 °C four seconds later. KSTAR operations are conservatively restricted to thermocouple temperatures below 600 °C, emphasizing the importance of effective heat management.

In KSTAR long-pulse discharges, the poloidal limiter showed more severe heating than the divertor. Even with diverted plasma shapes, limiter thermocouples frequently exceeded 600 °C within tens of seconds. This phenomenon was identified as being primarily caused by fast ion orbit losses from NBI. Simulations using the NuBDeC code demonstrated that different NBI sources contribute unequally to orbit losses, with NBI1-C responsible for  $\sim$ 38% of the total fast ions lost to the poloidal limiter, while NBI1-A contributed only  $\sim$ 19% and NBI1-B  $\sim$ 1%. The beam geometry of NBI1-C, with tangential radius Rtan = 1.23 m intersecting the inboard limiter, explains this unfavorable contribution. Thus, NBI1-C is unsuitable for long-pulse experiments where limiter protection is critical.

Plasma shape evolution further affects limiter heat loads. In discharge #21735, the outermost midplane radius ( $R_{out}$ ) increased nearly linearly from 2.21 m at 50 s to 2.27 m at 89 s, a drift attributed to signal errors in magnetic probes. This radial outward shift corresponded with increased fast ion loss to the poloidal limiter, further accelerating limiter heating after  $\sim$ 50 s. The correlation highlights the importance of controlling Rout within a threshold ( $\sim$ 2.21 m under these conditions) to minimize fast ion impact. Therefore, both beam source selection and plasma shape control must be integrated into the operational strategy for limiter protection.

In addition, the installation and operation of a tungsten monoblock divertor provided a robust engineering solution, enabling higher heat tolerance and improving the overall resilience of the divertor region under long-pulse conditions.

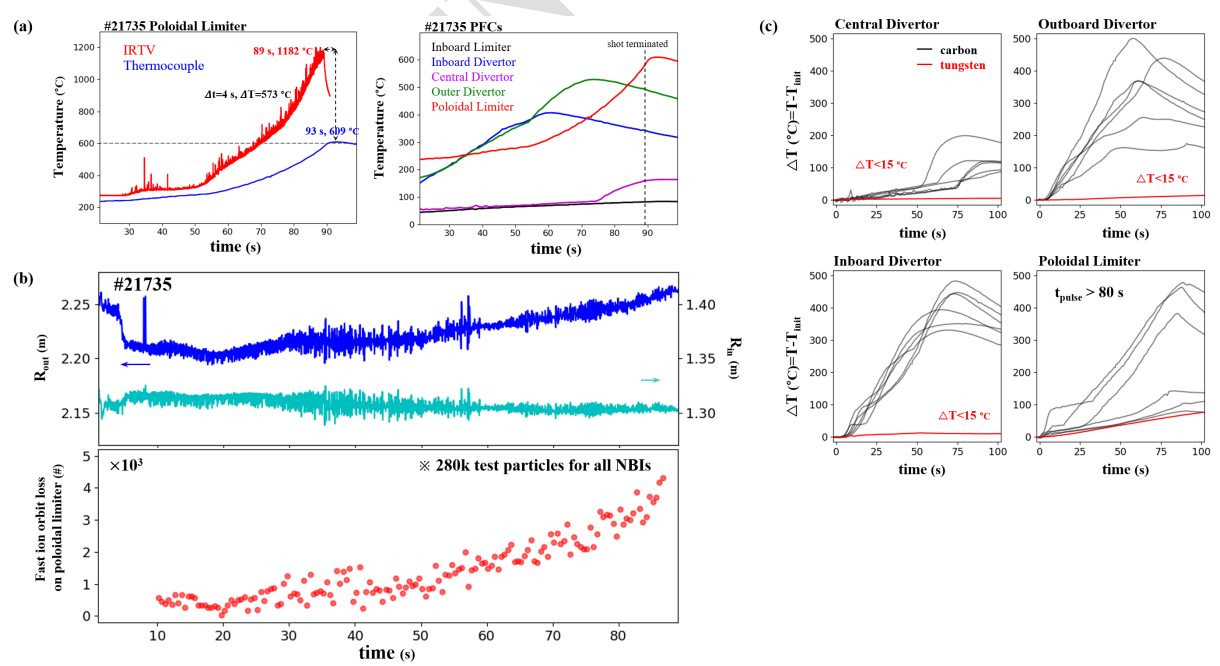


Fig. 2. (a) the temperature of the poloidal limiter measured by the IRTV (red) and the thermocouples (blue) and the temperature measured by the thermocouples for all the PFCs, (b) NuBDeC analysis of long-pulse discharge shows Rout and Rin of the plasma shape over time and the amount of fast ions lost to the poloidal limiter over time, and the temperature of the divertors by the installation of tungsten monoblock divertor.

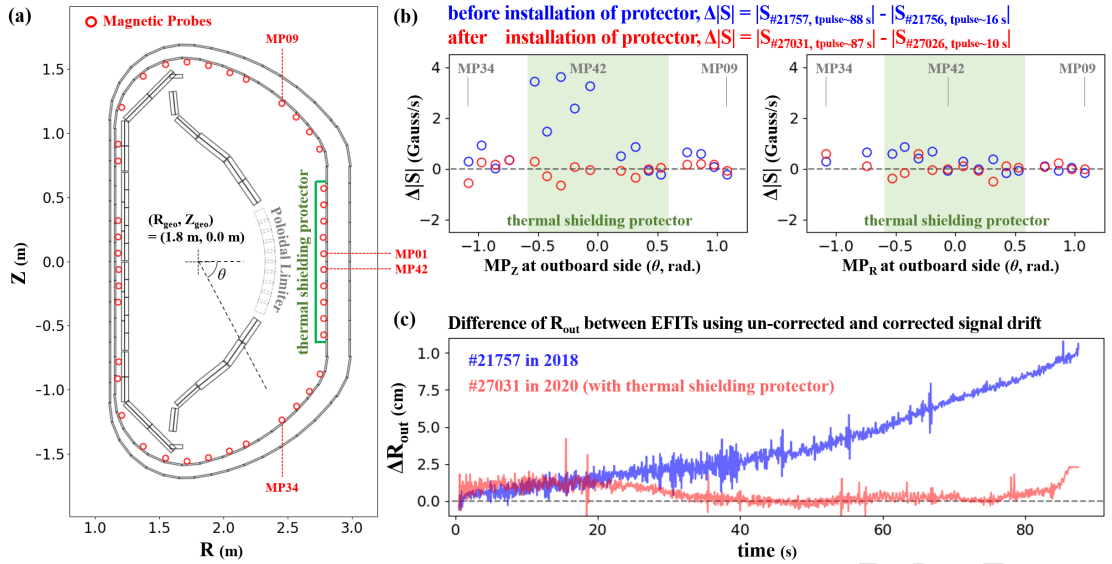


Fig. 3. Analysis of nonlinear signal drift from magnetic probes located on the outboard side of the plasma in the high-temperature long-pulse plasma operation. (a) describes a schematic cross-section of the KSTAR device, including the vessel, PFCs, and magnetic probes. In the KSTAR configuration, the PFC on the outboard side of the plasma in the midplane is open to the vessel. (b) presents the signal drift S analysis obtained from magnetic probes, MPZ and MPR, on the plasma outboard side at the midplane. (c) presents  $\Delta$ Rout obtained from EFIT analyses in long-pulse discharges.

#### 2.3. Mitigation of nonlinear signal drift in Magnetics

In the high-temperature and long-pulse plasma experiments conducted at KSTAR in 2018, significant nonlinear signal drift was observed in magnetic probes on the outboard side of the plasma. This drift was attributed to the accumulation of plasma heat transferred to the probes, associated with the temperature rise of plasma-facing components (PFCs). Such nonlinear drift reduced the accuracy and reliability of real-time plasma shape control. For example, in discharge #21735, although the actual outer radial position (Rout) increased over time, real-time EFIT erroneously maintained Rout at a constant value, which ultimately accelerated heating of the poloidal limiter. To mitigate this issue, a thermal shielding protector was installed on the magnetic probes in 2020.

The structural configuration of KSTAR exacerbated the problem. On the outboard side at the midplane, PFCs are open to the vacuum vessel, leaving the magnetic probes installed on the inner surface of the vessel directly exposed to vacuum and plasma. This exposure enhanced the transfer of plasma heat to the probes, thereby producing nonlinear signal drift that becomes more severe with longer pulse lengths. To quantify the effect, signal drift (S, in G/s) was evaluated using the probes MPZ and MPR, which measure the vertical and radial magnetic fields, respectively. The difference  $\Delta |S| = |S_{long}| - |S_{short}|$  was used to assess long-pulse effects beyond the inherent short-pulse drift. In 2018,  $\Delta |S|$  reached ~4.0 G/s, particularly in MPZ due to its coil orientation facing the plasma. In contrast, by 2020,  $\Delta |S|$  was effectively reduced to near zero, demonstrating the effectiveness of the thermal shielding protector.

The impact of nonlinear drift on equilibrium reconstruction was further evaluated by comparing EFIT analyses using drift-uncorrected and drift-corrected probe data. In discharge #21757 (2018), signal drift led to an apparent  $\Delta$ Rout of ~10 cm by the end of the pulse, whereas in discharge #27031 (2020),  $\Delta$ Rout was consistently  $\leq$ 1 cm. These results clearly demonstrate that the installation of the thermal shielding protector not only corrected the equilibrium reconstruction but also mitigated excessive heating of the poloidal limiter. Consequently, this improvement significantly enhanced the reliability of long-pulse plasma operation in KSTAR by ensuring accurate diagnostic performance under high-heat-load conditions.

In addtion, magnetic diagnostics are prone to signal drift, often exceeding the operational criterion of 0.3 mV/s per day and leading to distortions in real-time equilibrium reconstructions. Such drift cannot be fully recovered within the 12-minute inter-shot interval and is strongly dependent on discharge pulse length, though the baseline typically returns after overnight idle time. To overcome this limitation, we implemented a real-time linear drift correction method that determines slope and offset parameters from a reference discharge. The combined hardware stabilization and software compensation significantly reduced magnetic drift, achieving less than 2 cm plasma shape variation during a 102-second pulse. This correction operated continuously without interfering with genuine plasma responses and showed consistent performance across discharges. Overall, the successful operation of real-time linear drift correction establishes a robust framework for accurate magnetic equilibrium reconstruction and reliable plasma control.

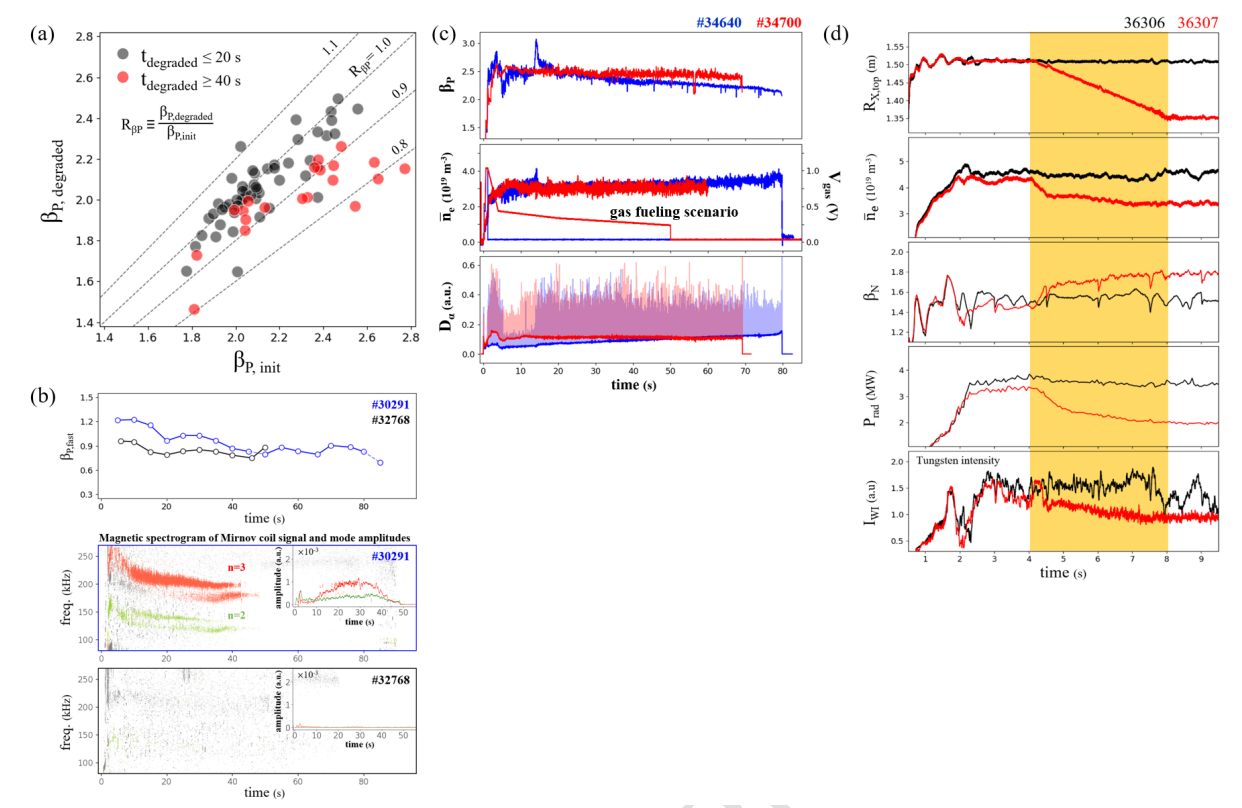


Fig. 4. (a)  $\beta_{P,init}$  versus  $\beta_{P,degraded}$  describing performance degradation over time, (b) comparison of  $\beta_{P,fast}$  and TAEs between discharges #30291 and #32768, (c) minimized performance degradation by optimized long-time scale gas fueling scenario, and (d) minimized radiative power in the condition of tungsten divertor by changing plasma shape.

### 2.4. Challenge of contant plasma perforamance in long-time scale

As described in figure 7, most of the KSTAR long-pulse discharges exhibited a gradual degradation of plasma performance. Figure 8 compares two representative cases with contrasting time evolutions. In discharge #30291,  $\beta$ P decreased almost linearly over time, showing an ~18% reduction by t~48 s despite constant external conditions. By contrast, discharge #32768 exhibited only a small initial drop for ~12 s, after which  $\beta$ P remained nearly constant with a minimal ~3% reduction until t~57 s. These distinct trends emphasize the need to identify the underlying mechanisms responsible for the observed degradation.

To investigate the performance differences, 0-D plasma characteristics were analyzed at 5 s intervals using the KSTAR kinetic-EFIT package with NUBEAM analysis. Both discharges were identified as typical H-mode plasmas with H98y2~1.1 and τΕ,th~42–52 ms, implying similar thermal confinement properties. However, while thermal stored energy (Wth) remained stable in both cases, significant differences were found in fast ion stored energy (Wf). In discharge #30291, the decrease in total stored energy (Wmhd) was mainly due to declining Wf, whereas in discharge #32768, Wf stayed nearly constant, consistent with its minimal degradation. This demonstrates that performance reduction in #30291 was dominated by fast ion pressure loss rather than thermal effects.

The decreasing trend of Wf in #30291 closely followed the neutron rate measured in the fission chamber, which aligned with NUBEAM-calculated neutron rates. This validates the reliability of the diagnostic and modeling tools used in the analysis. Moreover, density, core electron temperature at  $\psi N\sim0.1$ , and absorbed NBI power all remained stable, while Zeff showed little variation, indicating that the source population of fast ions was largely unchanged. Instead, the  $\sim$ 23% reduction in Wf (125  $\rightarrow$  96 kJ) correlated with the growth of the fast ion diffusion coefficient Df. Thus, the primary driver of performance degradation in #30291 was enhanced fast ion transport rather than changes in plasma source conditions.

The role of TAEs was then examined. Figure 10 shows that in discharge #30291, weak but persistent TAEs with n=2 (130–150 kHz) and n=3 (170–220 kHz) emerged during the degradation phase, with the n=3 TAE amplitude gradually increasing. By contrast, discharge #32768 showed no significant TAE activity, consistent with its stable performance. Comparison with high-performance discharge #27033 ( $\beta$ P~2.6) revealed n=2 TAEs of similar amplitude to those in #30291, but without a corresponding n=3 TAE. This suggests that the performance degradation in #30291 was likely associated with the excitation of the n=3 TAE, which enhanced fast ion transport

and reduced Wf. The absence of n=3 TAEs in #27033, despite similar  $\beta P$ , remains an open question requiring further study.

As noted earlier, the high βP scenario in KSTAR is based on precise ECH/ECCD control to suppress TAEs and improve fast ion confinement. In discharge #30291, early-phase operation (t≤8 s) successfully suppressed n=3 TAEs, consistent with the current relaxation time  $\tau R$  (~5 s). However, as the discharge evolved, fixed EC-wave deposition became less effective, and n=3 TAE activity reemerged with growing amplitude. This sustained TAE activity likely caused the observed reduction in fast ion pressure and  $\beta P$ . Notably, when  $\beta P$ , fast decreased to  $\sim 0.9$ , similar to discharge #32768, the n=3 TAE in #30291 stabilized beyond t~40 s. This time dependence underscores the importance of adaptive EC deposition strategies for long-pulse TAE control.

Figure 11 summarizes the overall characteristics of performance degradation in long-pulse experiments. Shorter discharges (tdegraded ≤20 s) maintained βP,based~1.8– 2.5 with minimal degradation (R $\beta$ P $\sim$ 0.9–1.1). Longer discharges (tdegraded ≥40 s) diverged into two groups: those with  $\beta P$ , based  $\leq 2.2$ maintained stability, while those with βP,based suffered degradation, ≥2.2 significant converging to βP,degraded~2.0–2.2. This convergence, highlighted by the shaded region in figure 11, strongly suggests that degradation severity increases with plasma performance level and is intimately linked to TAE dynamics, especially the excitation persistence of n=3 modes.

Firstly, to effectively control heat flux to the divertor and protect the inner walls of the device, KSTAR installed a W-shaped tungsten divertor capable of active water-cooling. The temperature variation measured by thermocouples on the tungsten divertor during the 102-second plasma was less than 15 °C, approximately 1/25th compared to previous long-pulse discharges. However, other PFCs excluding the tungsten divertor showed temperature variations of up to 100 °C. Secondly, an algorithm was successfully developed to real-time correction of the linear

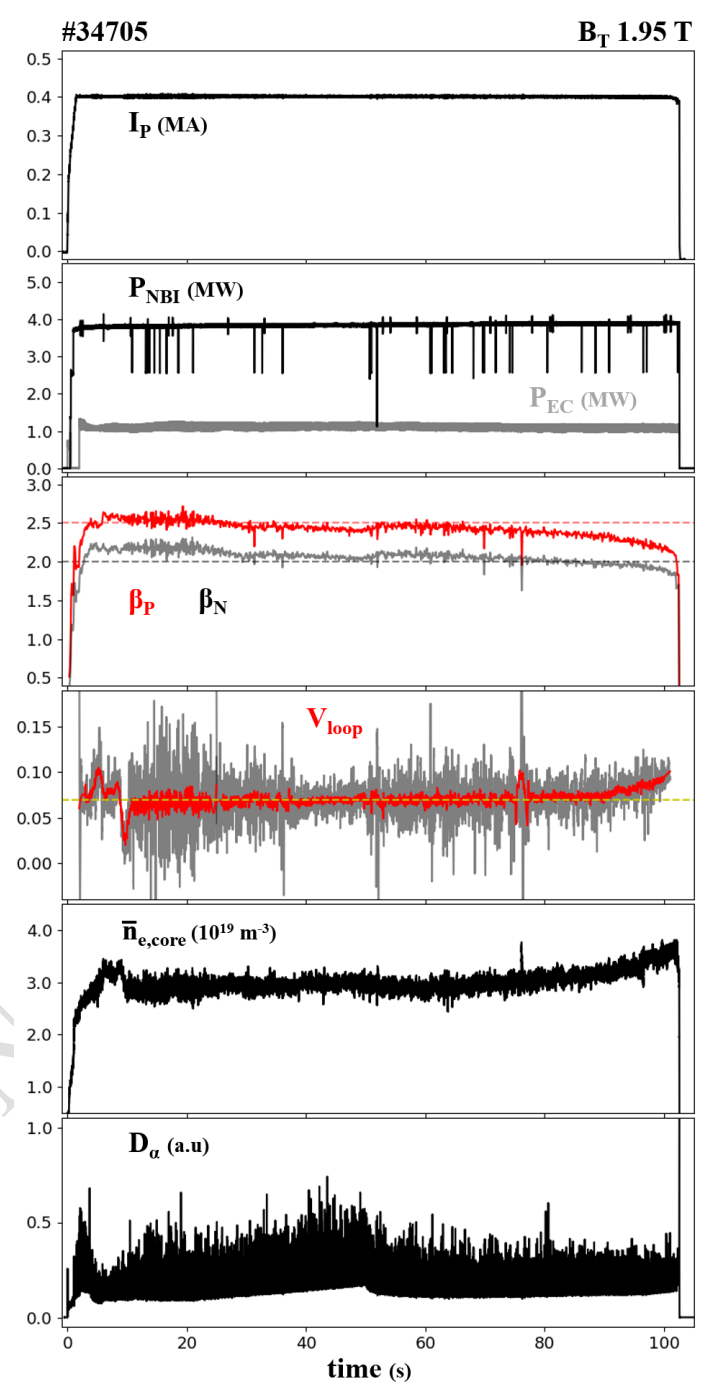


Fig. 5. 102-second high-performance long-pulse discharge in KSTAR in the condition of activly cooled tungsten divertor, real-time linear drift correction algorithm and themal shielding protector in magnetics, reoptimized shape scenario, and optimized long-time gas fueling scenario.

signal drift of magnetic diagnostics in PCS and applied to long-pulse plasma experiments. During the 102-second long-pulse plasma, key plasma shape variables were effectively controlled within a maximum error of 2 cm. Thirdly, to maintain a relatively low line-averaged electron density for lower loop voltage, the plasma shape scenario was updated. Changes in H-mode characteristics on the tungsten divertor environment were monitored due to changes in the plasma-facing material and divertor geometry, which influenced the plasma shape and the SOL region. Consequently, H-mode characteristics in the partially covered tungsten environment appeared to be significantly different from those in the previously fully covered carbon environment. In the H-mode plasma at IP=400-500 kA without additional gas injection, the line-averaged electron density was maintained at a higher value of ~4.0x1019 m-3 compared to previous discharges shown at ~2.0x1019 m-3. Additionally, the tungsten divertor led to the generation and accumulation of tungsten impurities, resulting in a 3-4 times increase in total

radiation power compared to before. In the case of the carbon divertor, the total power injection of ~5.0 MW resulted in the total radiation power of ~1.0 MW, whereas the tungsten divertor exhibited the total radiation power of ~3.0-4.0 MW. To enable long-pulse plasma operation, it was necessary to reduce plasma density and total radiation power by controlling the tungsten accumulation in the plasma, which was partially achieved by adjusting the plasma shape, especially the radial position of the inactive upper X-point (RX,top). As shown in Fig. 2, it was observed that as Rx,top decreases, plasma density, total radiation power, and tungsten intensity also decrease. We are still struggling with the detailed mechanism of this. Based on this result, the plasma shape scenario was optimized for long-pulse discharge. Fourthly, the phenomenon of gradual plasma performance degradation over time was significantly alleviated. The performance degradation that typically occurred around 20 seconds[2] was observed to be minimal up to approximately 70 seconds, where plasma performance remained almost constant. This is likely to have been influenced by changes in divertor geometry affecting the state of the SOL region and the appropriate scenario of gas injection.

The high-performance long-pulse discharges in KSTAR mostly operate in high  $\beta P$  mode, with Vloop~70 mV, fNI~0.70-0.75, and fBS~0.30-0.35. Under these plasma conditions, a pulse length of ~100 seconds is expected. To achieve and sustain the high-performance plasma state for 300 seconds, which is the mission goal in KSTAR, it is necessary to reach and maintain a nearly fully non-inductive plasma state with fNI  $\geq$  0.95. Based on collaborative research with DIII-D, we are developing a reproducible ITB (Internal Transport Barrier) formation scenario on KSTAR high  $\beta P$  mode. Additionally, since q-profile control is essential for sustaining long-duration ITB formation, we are experimentally investigating the q-profile response against KSTAR H&CD system.

This work is expected to contribute to the development of scenarios aimed at maintaining consistent plasma performance over time and monitoring the temperature behavior of PFCs during long-pulse plasma operation.

#### 3. SUMMARY AND PLANS

KSTAR aims to establish long-pulse operation of up to 300 seconds with high-performance plasma. To achieve this, two primary approaches have been emphasized: minimizing loop voltage (Vloop) and controlling the temperature rise of plasma-facing components (PFCs). Since neutral beam injection (NBI) is the primary heating and current drive (H&CD) system in KSTAR, understanding and controlling fast ion behavior is critical. Analyses revealed that fast ion orbit loss is strongly linked to the rapid temperature increase of the poloidal limiter as well as ~18% gradual plasma performance degradation. To address this, plasma shape optimization, selective use of NBI sources, and control of strike point locations were implemented. In particular, excluding the NBI1-C source effectively reduced heating not only of the poloidal limiter but also of the inboard limiter, which was susceptible to beam shine-through. The application of electron cyclotron heating (ECH) further reduced Vloop to ~25 mV by enhancing NBI-driven current through electron heating. Additionally, ECH/ECCD provided stabilization of toroidal Alfvén eigenmodes (TAEs), thereby improving fast ion confinement and contributing to sustained high βP operation.

With these optimized techniques, KSTAR achieved ~90-second long-pulse discharges under the conditions of IP=400 kA, BT~1.8–2.5 T, PNBI $\leq$ 5.2 MW, and PECH $\leq$ 1.4 MW. The resulting plasma parameters were (ne) $\leq$ 2.8×1019 m-3, Te,core $\leq$ 5.0 keV, Ti,core~2.0 keV,  $\beta$ P $\leq$ 2.7, H98y2~1.1, Vloop~34–100 mV, and fNI~0.69–0.96 with bootstrap fraction fBS~0.29–0.37 and externally driven current fraction fCD~0.40–0.59. To enhance diagnostic reliability, nonlinear signal drift in magnetic probes—caused by accumulated heating—was addressed by installing thermal shielding protectors, which successfully improved EFIT accuracy and real-time plasma shape control. These integrated strategies enabled stable long-pulse performance while mitigating engineering and physics-related risks.

Nevertheless, plasma performance degradation persisted over longer timescales. Detailed analysis showed that the decrease in total stored energy originated primarily from reductions in fast ion stored energy, not thermal energy. This degradation correlated with anomalous increases in fast ion diffusion coefficients, reduced neutron rates, and the emergence of low-amplitude yet sustained TAEs. Although precise ECH/ECCD deposition effectively suppressed TAEs during the early discharge phase ( $t \le 8$  s), their amplitudes later grew under evolving plasma conditions, leading to reduced fast ion pressure. As the pulse length exceeded 40 seconds,  $\beta P$  consistently converged toward  $\sim 2.0-2.2$ , suggesting that performance degradation was closely coupled with TAE activity. Future investigations with FIDA diagnostics and NOVA-k modeling are planned to clarify the physical mechanisms linking fast ion transport, TAEs, and long-timescale performance degradation in KSTAR.

If you need to subdivide the sections of your paper, use the headings shown below. You can use second and third level paper headings. To subdivide further, please use lists numbered (a), (b), and so on, but this is usually not necessary in a paper of normal length.

#### **ACKNOWLEDGEMENTS**

This research was supported by the R&D Program of "High Performance Tokamak Plasma Research & Development (EN2501-16)" through the Korea Institute of Fusion Energy (KFE) funded by the Government funds, Republic of Korea.

#### REFERENCES

- [1] AUTHOR, A., Book Title in Title Case, Series No. if applicable, Publisher, Place of Publication (Year).
- [2] AUTHOR, A., Internal Report Title in Title Case, internal report, Organization, Location, Year.
- [3] LETTER-WRITER, A., Organization, personal communication, Year.
- [4] RESEARCHER, A., Organization, unpublished data.
- [5] CHAPTER-AUTHOR, A., "Title of chapter in sentence case", Book Title in Title Case, Publisher, Place of Publication (Year).
- [6] AUTHOR, A., AUTHOR, B., AUTHOR, C., Journal article title in sentence case, Abb. J. Title 1 2 (Year) 120-123.
- [7] AUTHOR, A., Title of Web Page or On-line Database in Title Case (Year), www.webpage.com/exact-subpage-being-cited
- [8] AUTHOR, A., "Paper title in sentence case", Conference Title in Title Case (Proc. Int. Conf. Place of Conference, year), Publisher, Place of Publication (Year).
- [9] PRESENTER, A., "Title of presentation in sentence case", Paper No., paper presented at Organization seminar on subject, Location, year.
- [10] Title of INFCIRC in Title Case, INFCIRC No., IAEA, Vienna (Year).